Self-Assembly of Semiconductor Organogelator Nanowires for Photoinduced Charge Separation

André Wicklein,[†] Suhrit Ghosh,[‡] Michael Sommer,[†] Frank Würthner,[‡,*] and Mukundan Thelakkat[†,*]

[†]University of Bayreuth, Macromolecular Chemistry I—Applied Functional Polymers, Universitätsstrasse 30, 95440 Bayreuth, Germany, and [‡]Universität Würzburg, Institut für Organische Chemie, Am Hubland, 97074 Würzburg, Germany

ABSTRACT We investigated an innovative concept of general validity based on an organogel/polymer system to generate donor—acceptor nanostructures suitable for charge generation and charge transport. An electron conducting (acceptor) perylene bisimide organogelator forms nanowires in suitable solvents during gelation process. This phenomenon was utilized for its self-assembly in an amorphous hole conducting (donor) polymer matrix to realize an interpenetrating donor—acceptor interface with inherent morphological stability. The self-assembly and interface generation were carried out either stepwise or in a single-step. Morphology of the donor—acceptor network in thin films obtained *via* both routes were studied by a combination of scanning electron microscopy and atomic force microscopy. Additionally, photoinduced charge separation and charge transport in these systems were tested in organic solar cells. Fabrication steps of multilayer organogel/polymer photovoltaic devices were optimized with respect to morphology and surface roughness by introducing additional smoothening layers and charge injection/blocking layers. An inverted cell geometry was used here in which electrons are collected at the bottom electrode and holes at the top electrode. The simultaneous preparation of the interface exhibits almost 3-fold improvement in device characteristics compared to the successive method. The device characteristics under AM1.5 spectral conditions and 100 mW/cm^2 for the simultaneous preparation route are short circuit current $J_{sc} = 0.28$ mAcm^{-2}, open circuit voltage $V_{0C} = 390$ mV, fill factor FF = 38%, and a power conversion efficiency $\eta = 0.041\%$.

KEYWORDS: donor—acceptor heterojunction · nanostructure · self-assembly · organogelator · photovoltaic devices · solar cells

Electronic devices made of organic materials, in particular photovoltaic devices, were intensively studied during the last years owing to their potential regarding cheap processing costs, their application to large areas, and their compatibility with flexible substrates.[1,2] In organic solar cells, charge separation of the strongly bound electron-hole pairs, so called excitons is enabled at a donor-acceptor (DA) interface or heterojunction upon illumination, where they dissociate and then drift towards the respective electrodes. For an ideal heterojunction, an interpenetrating network between an electron-acceptor and -donor material with a suitable concentration gradient in the two materials towards the respective charge collecting electrodes is the most ideal one. This led to the introduction of the bulk heterojunction concept.[3−5] There are different approaches to generate organic bulk heterojunctions. Blending donor and acceptor components has led to highly efficient solar cell systems, even though the desired stable bicontinuous morpholgy in the nanometer scale in entire bulk is still difficult to achieve.[6] It is desirable not only to match the domain size of the components and the exciton diffusion length, but also to obtain equilibrium nanostructures which assure morphological and device stability. Therefore, generating "nanostructured bulk heterojunctions" that guarantee an adequate percolation of charges is the ultimate goal. One of the ways to accomplish this task has already been demonstrated by some of us, in which equilibrium nanostructures have been realized using self-organization of semiconductor diblock copolymers.[7,8] Other concepts include so-called double cable polymers[9] and supramolecular p−n heterojunctions.[10−13]

Organogelators in general form physical networks originating from nanostructures, extending over large area and volume.[14−17] The self-assembly process of gelators results in the formation of one-dimensional supramolecular fibers that are bundled up together and entangled at nodes to form a complex fibrous three-dimensional physical network. The solvent molecules are entrapped by this network that interlaces the whole system. These unique structural features are more or less maintained in the xerogel, obtained after the removal of the solvent, if sudden aggregation leading to loss of structures during drying is avoided. The fundamental question in this work is whether this supramolecular approach can be elegantly realized using an acceptor-type organogelator, which can then be

*Address correspondence to mukundan.thelakkat@uni-bayreuth.de, wuerthner@chemie.uni-wuerzburg.de.

Received for review February 5, 2009 and accepted April 15, 2009.

Published online May 1, 2009.
10.1021/nn9001165 CCC: $40.75

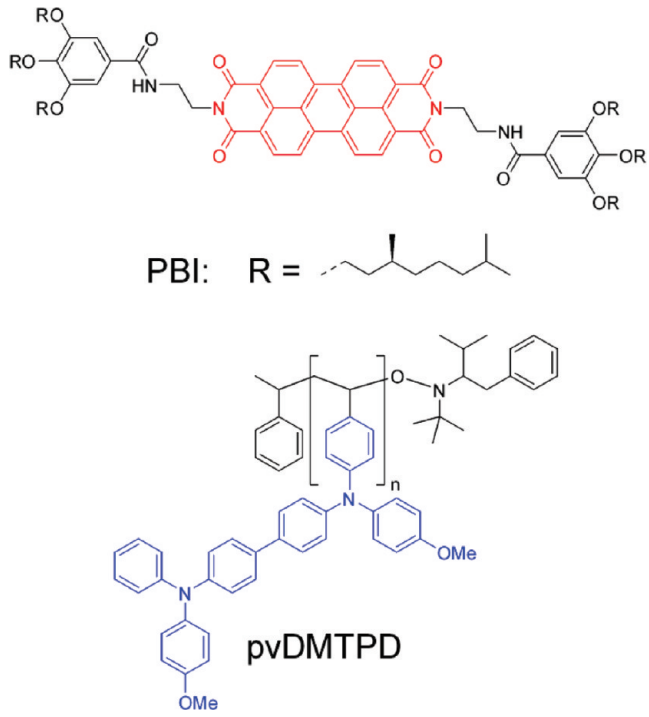

Figure 1. Molecular structures of perylene bisimide organogelator PBI, and hole-transporting polymer poly{*N,N*′-bis(4-methoxyphenyl)-*N*-phenyl-*N*′-4-vinylphenyl-[1,1′-biphenyl]-4,4′-diamin} *p*vDMTPD.

embedded into a donor-type matrix or vice versa. Such a self-organized, nanostructured functional material incorporated into another functional material, without hindering the self-assembly process to a large extent, would provide a large interface area suitable for charge separation. It also provides charge percolation pathways on the nanometer scale. Perylene bisimides (PBI) are excellent electron conducting (acceptor) dyes exhibiting high charge carrier mobility.[18] Similarly there are a variety of hole conductor materials (donors) such as tetraphenyl benzidines,[19] conjugated polymers[20] with high charge carrier mobility. It is also worthy to note that photoinduced charge separation in general has already been reported in perylene bisimide−hole conductor polymer blend systems.[21−23] Organogelators have also been successfully employed in quasi-solid-state dye sensitized solar cells in order to gelate the liquid electrolyte. Here the organogelators do not have any electronic functions suitable for charge separation and charge transport.[24,25] But a direct use of a semiconducting organogel as active material in donor−acceptor systems is not yet reported.

On the basis of this idea we describe here an innovative novel concept to create a nanostructured donor−acceptor interface by combining hydrogen bond-directed self-assembly of an n-type organogelator, perylene bisimide (PBI)[26,27] with a p-type polymer, poly(vinyl-dimethoxytetraphenylbenzidine) (*p*vDMTPD)[28] (Figure 1). Because of noncovalent hydrogen-bonding and π−π-stacking interactions, the PBI organogelator forms well-defined π-stacks with favorable *J*-type packing of the dyes.[26] AFM height image of semiconductor nanowires as formed by spin-coating from diluted gel solutions of PBI in methylcyclohexane onto HOPG substrate is shown in Figure 2a. These *J*-type PBI π-stacks are almost black and accordingly act as efficient light harvesting moieties over the whole visible range. To verify the utility of this approach, prototype organogel/polymer solar cells were also prepared and characterized. A detailed characterization of morphology of the donor−acceptor system using SEM and AFM was also carried out.

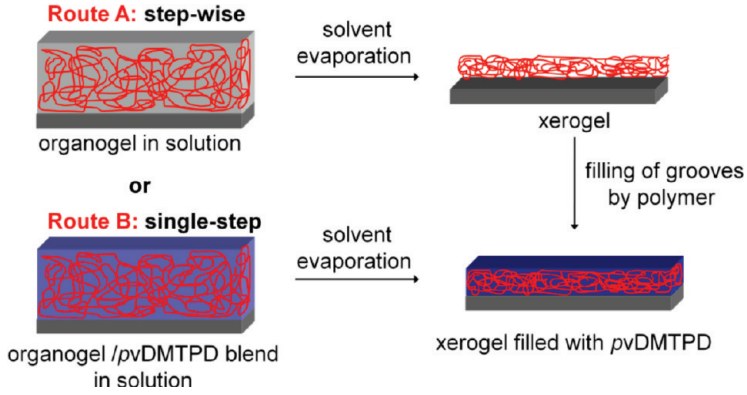

Figure 2. Schematic representation of organogel-polymer concept for realization of an interpenetrating organic bulk heterojunction. Route A: formation of n-type xerogel with subsequent filling with p-type polymer. Route B: concomitant embedding of the physical network by a blend approach.

RESULTS AND DISCUSSION

We prepared the gelated network by two different methods (Figure 2). Route A is a step-wise method of preparation of PBI−organogel followed by removal of solvent (leading to xerogel) and subsequent filling of pores and grooves by using *p*vDMTPD, and route B is a single-step method of simultaneous formation of a three-dimensional physical network of PBI−organogel embedded into amorphous *p*vDMTPD matrix by a blend approach. The details of preparation of the xerogel, donor−acceptor interpenetrating network, its optimization to get smooth films suitable for device preparation, and device characteristics are discussed below.

For the realization of working devices it is of extreme importance to use smooth films of high optical quality. This guarantees good contacts at organic−metal interfaces resulting in efficient charge extraction. With this in mind we tried different solvents, such as methylcyclohexane, chlorobenzene, toluene, and $CHCl_3$ for the preparation of gelated layers in devices. Since PBI is not soluble enough at room temperature, hot solutions in these solvents were used to optimize film formation. The films from hot chlorobenzene solution resulted in coarse gel structures not suitable for blend heterojunction. Only by using 2.0 wt % $CHCl_3$, high optical quality films for both routes A and B were obtained. And therefore

$CHCl_3$ solutions were used for further optimization and characterization. For film preparation we used a doctor-blading technique, in which different film applicator blades, such as spiral blade or quadruple blade were drawn over a concentrated solution of the material placed on a substrate. The use of spiral applicator blade delivered the desired uniform films suitable for device preparation. In route A, thin films of PBI−xerogel were prepared from hot, 2.0 wt % $CHCl_3$ solution onto fluorine-doped tin oxide (FTO) glass substrates. Initially a thin gel film is formed which upon solvent evaporation subsequently shrinks to develop the xerogel-structure. A striking advantage of PBI−xerogel is that the xerogel-network is almost insoluble in $CHCl_3$ at room temperature and therefore suited for filling by *pv*DMTPD, by using solution processing, in a subsequent step. For route B, blends of PBI:*pv*DMTPD in different compositions, B1 = 3:1, B2 = 1:1, and B3 = 1:3 weight percentages, respectively, were prepared in $CHCl_3$, and films of different thicknesses were prepared by doctor-blading. As shown later (solar cell discussion), the blend with 3:1 (PBI:*pv*DMTPD) composition delivered highest current and power conversion values. Therefore, for a comparison of film morphologies obtained *via* route A and route B, only this blend composition B1 (3:1) is taken as a typical example here. For both routes, the doctor-blading technique is essential for the formation of an extensive and continuous network in thin films. The organogel acceptor molecule builds nanostructures in solution as well as in the donor polymer blend. These structural features aggregate during drying in both routes A and B, but still result in a large area of donor−acceptor interface suitable for charge separation and charge transport.

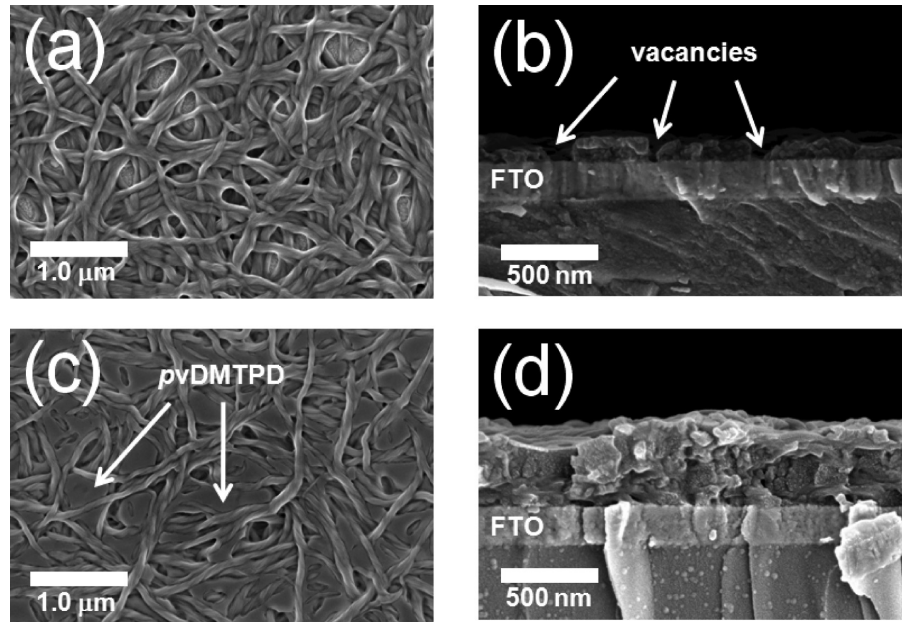

Figure 3. SEM surface images of (a) PBI−xerogel *via* route A and (b) corresponding cross section. (c) Surface image of PBI−xerogel/*pv*DMTPD blend (3:1) *via* route B and (d) corresponding cross section. The hole-transporting polymer *pv*DMTPD acts as filler for the interstitial volume in the xerogel. Films were prepared by doctor-blading technique from hot (55 °C) 2.0 wt % $CHCl_3$ solutions.

Figure 3 shows scanning electron microscopy (SEM) images of the PBI−xerogel (Figure 3a,b) and the PBI−xerogel/*pv*DMTPD (3:1) blend (Figure 3c,d). The superstructure of PBI−xerogel consists of twisted strands of about 50 nm thickness which are entangled. Thus the

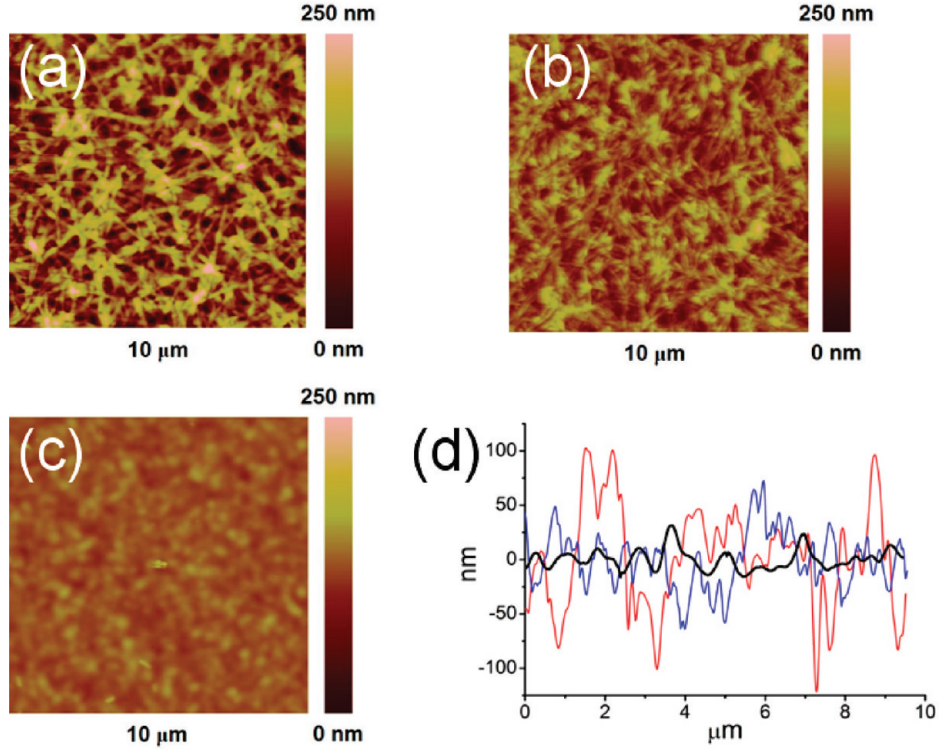

Figure 4. AFM height-images of (a) PBI−xerogel *via* route A, (b) PBI−xerogel/*pv*DMTPD blend (3:1) *via* route B, (c) corresponding PBI−xerogel/*pv*DMTPD blend (3:1) with additional overstanding *pv*DMTPD layer, scale 0−250 nm; (d) respective topography cross sections of PBI−xerogel (red), PBI−xerogel/*pv*DMTPD blend (3:1) (blue), and PBI−xerogel/*pv*DMTPD blend (3:1) with additional overstanding *pv*DMTPD layer (black).

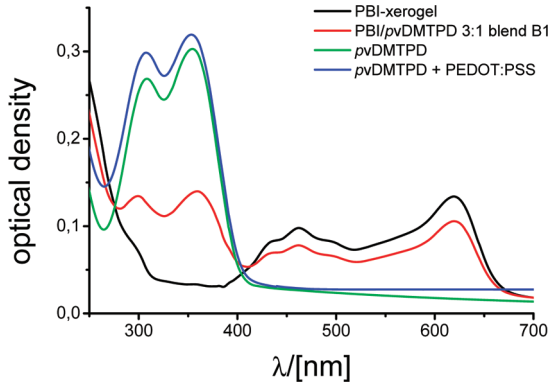

Figure 5. UV−vis absorption spectra of individual layers and blend films. The films were prepared on quartz substrates by doctor-blading using the same conditions as those used in solar cell preparation. The film thicknesses correspond to the respective thicknesses in solar cell devices. *p*vDMTPD layer was prepared from 5.0 wt % chlorobenzene solution, whereas the blend B1 (3:1) as well as PBI−xerogel layers were prepared from 2.0 wt % hot chloroform solution.

real morphology available for device preparation in thin films is strongly aggregated compared to the individual PBI-strands observed in dilute solutions. Even though the PBI nanofiber morphology formed in dilute solutions is metastable and can aggregate over time,[29,30] the drying process in route A to obtain the xerogel and the blending process in route B to fix the xerogel network in a polymer matrix allow us to freeze the partially aggregated morphology as seen in SEM of thin films. The xerogel with its nanometer sized grooves exhibits enough interstitial volume for filling with the hole-transport polymer. It can clearly be seen from Figure 3c,d that the amorphous polymer *p*vDMTPD fills very efficiently the vacancies in the xerogel in the case of the blend film obtained *via* route B. Nevertheless, there are still some voids observable in Figure 3c, requiring an additional overstanding hole conductor *p*vDMTPD layer to guarantee smooth contacts with top electrode (see AFM results, Figure 4). Furthermore the polymer chains hinder individual gel-strands from additional sticking or collapsing compared to the pure xerogel which forms thicker strands. This also leads to an increased interface area between electron-donor and acceptor material in route B, compared to that in route A.

The topography of the films obtained by both routes was also examined by atomic force microscopy (AFM) measurements. The surface of both films revealed a high roughness as seen in Figure 4a,b. The roughness of PBI−xerogel/*p*vDMTPD 3:1 blend film is less compared to pure PBI−xerogel film (Figure 4d). This is due to a partial filling of the xerogel by the amorphous polymer in blend films. Even then such rough surfaces are not suitable for evaporation of metal-electrodes on top and therefore an additional smoothening layer is necessary. Thus overstanding *p*vDMTPD layers were prepared on top in both cases before gold deposition, not only to smoothen the rough surface in all cases, but also to fill cavities in the xerogel film. To this end, *p*vDMTPD solution in chlorobenzene was doctor-bladed resulting in an overstanding hole-transporting layer of 150 nm thickness. The smoothening effect can be observed clearly in Figure 4c, in which the average roughness of the films is drastically reduced (Figure. 4d). This overstanding layer has an additional electron-blocking function in devices, which helps to avoid direct contact of electron conducting PBI and hole collecting gold electrode on the top. For device preparation an additional hole injection layer of highly conducting poly(3,4-ethylenedioxythiophene)/poly(styrene sulfonate) (PEDOT:PSS) was coated on top of the *p*vDMTPD layer to improve the contact between *p*vDMTPD and gold.

A fundamental question regarding light harvesting in multilayer devices is the individual contributions of each layer toward absorption. This can be studied by comparing the absorption spectra of individual layers in such a device. Figure 5 compares the absorption spectra of pure PBI−xerogel, pure *p*vDMTPD, *p*vDMTPD with PEDOT:PSS on top and a 3:1 blend of PBI/*p*vDMTPD as prepared on quartz substrates. The hole transport polymer *p*vDMTPD absorbs up to 400 nm, whereas gelated PBI absorbs mainly in the region between 400 and 650 nm. The contribution of PEDOT:PSS toward absorption in these devices is negligible as observed by the comparison of the absorption spectra of *p*vDMTPD with or without PEDOT:PSS layer.

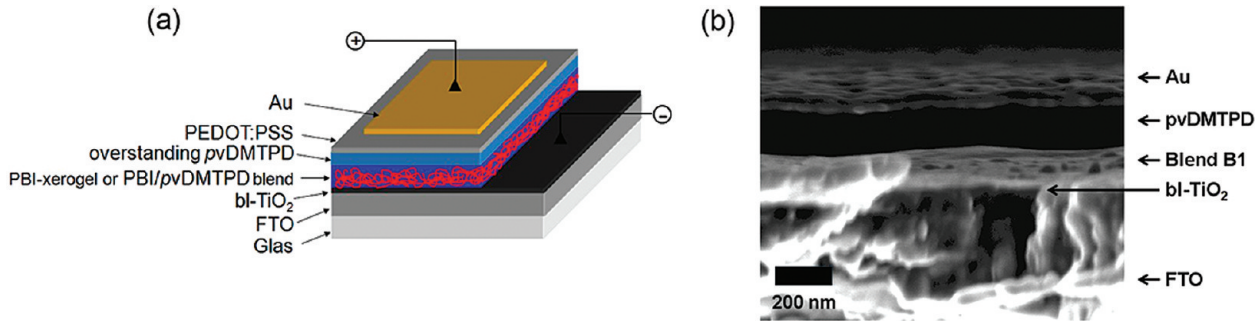

Figure 6. (a) General device architecture with inverted cell configuration. FTO = Flourine doped tin oxide, PEDOT = poly(3,4-ethylenedioxythiophene), PSS = poly(styrene sulfonate). (b) SEM cross section of a typical blend device B1 prepared *via* route B.

TABLE 1. Photovoltaic Characteristics of Different Photovoltaic Devices Employing the Organogel/Polymer Concept *via* Routes A and B

cell	blend composition PBI:*pv*DMTPD	J_{SC} [mA/cm^2]	V_{OC} [mV]	FF [%]	η [%]
device B1	3: 1	0.28	390	38	0.041
device B2	1:1	0.27	350	35	0.033
device B3	1:3	0.23	300	36	0.024
device A	-	0.18	210	41	0.015

This is also the reason why PEDOT:PSS is used as a common charge injection layer for holes without any adverse effect on the transmission property of the electrode used. The absorption spectra of PBI/*pv*DMTPD 3:1 blend film is a superposition of the individual absorption spectra indicating no charge-transfer in the ground-state. Additionally, both PBI and blend spectra show the characteristic *J*-type absorption peaks of PBI nanofibers at 619 nm and at 462 nm.[26] Thus, in both systems efficient light harvesting in the range of 400 to 650 nm is guaranteed by the broad absorption band of the black PBI organogelator and below 400 nm by *pv*DMTPD.

To elucidate the photoinduced charge-separation in organogel/polymer systems, first the influence of PBI:*pv*DMTPD composition on solar cell performance was studied. Three different PBI:*pv*DMTPD blend compositions, B1 = 3:1, B2 = 1:1, and B3 = 1:3 weight percentages, respectively, were prepared and integrated into solar cells using route B. Figure 6a represents schematically the device structure and Figure 6b a typical SEM cross section for blend B1 (3:1). Here the individual layers of such a device can be observed clearly. No remarkable differences could be observed in SEM cross sections of B1, B2, and B3.

With the optimized conditions of film preparation the photovoltaic devices were prepared. Because an overstanding hole-transporting layer is essential in these devices, an inverted cell configuration with an electron collecting electrode at the bottom (FTO) and a hole-collecting electrode (Au) at the top was utilized (Figure 6a). The general device structure is FTO/bl-TiO_2/PBI−xerogel:*pv*DMTPD blend/*pv*DMTPD /PEDOT:PSS/Au. Any contact between hole conducting *pv*DMTPD and FTO electrode leads to significant loss of current in photovoltaic devices. Hence an additional TiO_2 blocking layer (bl-TiO_2) onto the FTO-layer is essential to avoid short-circuiting and loss of current through recombination between FTO and *pv*DMTPD. To ensure uniform film thickness for the bl-TiO_2 layer, an automated method of preparation of such a compact layer of TiO_2 starting from titanium(IV)bis(acetoacetonato)-di(isopropanoxylate) (TAA) by spray pyrolysis deposition, which was developed in our laboratories, was used here.[31] Also an additional injection layer of PEDOT:PSS was coated on top. Gold electrodes were evaporated on top of the active layers by vacuum deposition at 10^{-6} mbar. The active area of a single device was 0.12 cm^2. These double-layer devices were characterized by means of current−voltage measurements in the dark and under illumination with a calibrated AM1.5 white-light source. All measurements and preparation steps were performed at ambient conditions without any encapsulation or protection of the devices against degradation (see Methods section for details).

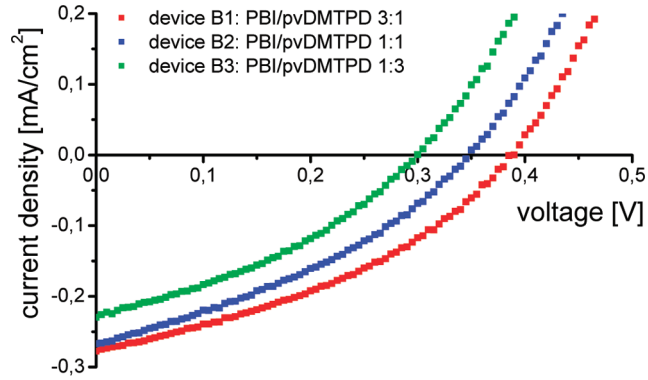

Figure 7. Plot of current density (*J*) *versus* voltage (*V*) under illumination with white light (AM 1.5 spectral conditions, 100 mW cm^{-2}) for photovoltaic devices constructed from PBI−xerogel/pvDMTPD blend with an additional overstanding pvDMTPD layer. The compositions for the devices B1, B2, and B3 are 3:1, 1:1, and 1:3 (PBI:*pv*DMTPD wt %), respectively.

In the following the results of the three different blend cells are discussed first. The overall solar cell parameters for all devices are given in Table 1. The current−voltage characteristics of the three blend solar cells are depicted in Figure 7. All devices deliver appreciable photocurrent and photovoltage, demonstrating the presence of percolation paths for photogenerated electrons and holes in organogel−polymer composite material. The B3 (1:3) blend delivers the smallest photocurrent and photovoltage, whereas the blend B1 (3:1) gives the best performance. The performance of blend B2 (1:1) lies in between B1 and B3. Thus blend B1 gives a short-circuit current density (J_{SC}) of 0.28 mAcm^{-2}, an open-circuit voltage (U_{OC}) of 390 mV, a fill factor (FF) of 38% and a power conversion efficiency of 0.04%. The highest current observed in device B1 is due to better light-harvesting in the 400−650 nm region, due to increased PBI−chromophore content in blend B1. A further improvement in overall light-harvesting and efficieny can be achieved by increasing the perylene content in the organogelator. For the discussion of the two different routes (A,B) of device preparation, only the best performing blend device B1 will be considered further.

An exact control test using nongelated PBI under the same conditions of film and device preparation as that for the gelated system in order to understand the importance of network structure toward charge-separation and charge-transport is extremely difficult to realize. This was because the used PBI gelated ex-

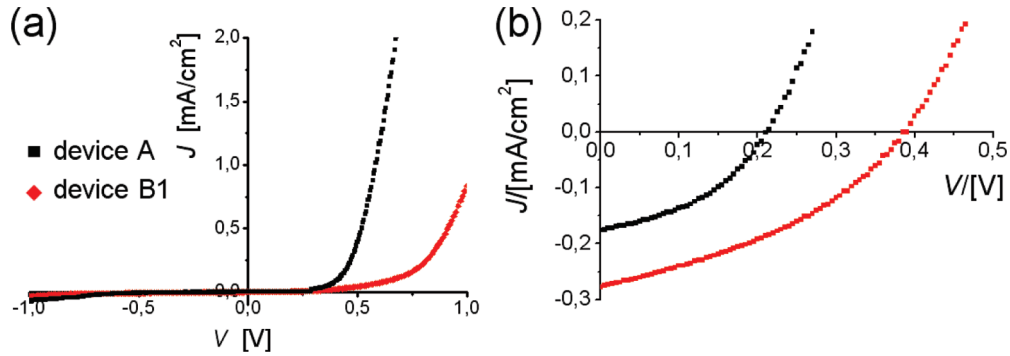

Figure 8. Plots of current density (*J*) *versus* voltage (*V*) for photovoltaic devices constructed from PBI−xerogel device A (black) and PBI−xerogel/*pv*DMTPD blend B1 (3:1) device B1 (red). (a) Measurements under dark and (b) under illumination with AM 1.5 spectral conditions and 100 mW cm^{-2}. The short circuit current (J_{sc}) and the open circuit voltage (V_{oc}) are 0.18 mA cm^{-2} and 210 mV for the device A and 0.28 mA cm^{-2} and 390 mV for the device B1, respectively. The power conversion efficiency could also be improved from 0.015% for device A to 0.041% for device B1.

tremely fast in solvents suitable for film preparation; since PBI exists in nongelated form only in hot solutions and during film preparation it suddenly forms the gel network with different degrees of agglomeration. Therefore, a control experiment with an electronically similar, highly soluble, and nongelating PBI derivative, *N*-(1-nonyldecyl)-*N*′-(1-pentylhexyl)-perylene-3,4,9,10-tetracarboxylic bisimide in combination with *pv*DMTPD, was performed. This control device delivered very low current, voltage, and overall efficiency values (J_{SC} = 0.04 mAcm^{-2}, V_{OC} = 275 mV, FF = 33%, η = 0.003%) compared to all the three blend devices. This clearly supports the necessity of an interpenetrating donor−acceptor network as in organogel/polymer systems for efficient charge separation and charge transport. This is in full agreement with reports in the literature regarding bulk-heterojunction devices *versus* devices lacking interpenetrating networks.[3,7]

Finally the efficacy of route A (stepwise method) was compared with that of route B (single-step method), using the best blend composition B1 (3:1). Device A (FTO/bl-TiO_2/PBI−xerogel/*pv*DMTPD/PEDOT:PSS/Au) follows route A using PBI−xerogel subsequently filled up with *pv*DMTPD. The device B1 has the structure, FTO/bl-TiO_2/PBI−xerogel:*pv*DMTPD blend (3:1)/*pv*DMTPD/PEDOT:PSS/Au). Figure 8a,b compares the current−voltage characteristics of devices A and B1 measured in the dark and under illumination. PBI−xerogel/pvDMTPD (3:1) blend device B1 works significantly better than the PBI−xerogel device A. The short circuit current J_{sc} is 0.18 mA cm^{-2} and 0.28 mA cm^{-2} for the device A and B1 respectively. The open circuit voltage V_{oc} increases from 210 mV for device A to 390 mV for the device B1. The fill factors are 41% and 38% for device A and B1 respectively. Accordingly the power conversion efficiency η is improved by a factor of almost three from 0.015% for device A to 0.041% for device B1. It is also worthy to note that all the devices prepared *via* route B (B1, B2 and B3) perform better than device A. On comparison of devices A and B1, both having similar optical density resulting in similar light-harvesting, the difference in performance can only be attributed to the difference in interface area as well as morphology in the active layer. In route A the xerogel was prepared in the absence of *pv*DMTPD, whereas in route B the drying process took place in the presence of matrix polymer. This can lead to better contact between gel fibers and polymer in device B1.

The generally observed low current values for these organogel/polymer devices are in accordance with the very low optical density in these devices (<0.15 in the range of 400−650 nm), which has to be improved considerably for efficient light-harvesting. A further elaborate fine-tuning of the relative thicknesses of each individual layer and device preparation conditions under inert atmosphere may also be required to improve the performance. It is noteworthy that both devices are quite stable against degradation with only a small loss in fill factor after several weeks. Both J_{SC} and V_{OC} remained constant for 8 weeks.

The performance of reported blend devices prepared from conjugated p-type polymers and low molecular weight PBIs, reported up to now exhibit very low photocurrent and efficiency.[21−23] These state of the art blend systems suffer from crystallization of perylene bisimides and lack of nanostructured interpenetrating networks. Even though the absolute values reported here are not comparable to the highly optimized blend systems using polythiophene and fullerene, the performance of our organogel/polymer devices can be improved by increasing the active amount of chromophore content as well as using better hole transport conjugated polymers. Future investigations will be directed toward this by developing PBI organogelators bearing smaller substituents at the imide nitrogen which increases the chromophore content resulting in higher optical densities and better charge transport properties. One important advantage of this concept is the possible morphological stability of this system guaranteed *via* the insoluble xerogel network frozen into a polymer matrix, which avoids the diffusion of molecules and large scale macrophase separation.

CONCLUSIONS

To conclude, we could provide an innovative and simple donor−acceptor heterojunction concept utilizing the self-assembly principle of a low molecular weight organogelator in the presence of an amorphous hole conductor polymer. The organogel acceptor molecule builds nanostructures in the presence of the donor polymer resulting in a large area of donor−acceptor interface suitable for charge separation and charge transport. This is a universal approach to use blends of functional gelators in combination with complementary semiconductor polymers. Also a proof-of-principle for application in organic solar cells is given. This concept has great potentials of improvement by utilizing low band gap conjugated polymers and organogelators that combine favorable absorption properties and high charge carrier mobilities. This is a conceptual novelty in the field of nanostructured donor−acceptor bulk heterojunction.

METHODS

The synthetic details of the preparation of PBI-organogelator[26,27] and poly(vinyl-dimethoxytetraphenylbenzidine) (*p*vDMTPD)[28] were reported elsewhere. Titanium(IV)bis(acetoacetonato)-di(isopropanoxylate) (TAA) and PEDOT/PSS dispersion were purchased (Aldrich) and used as received. Glass substrates (Tec 8) covered with ~3 mm fluorine-doped tin oxide (FTO) layer having a sheet resistance of 8 Ω per square were purchased from Hartford Glass Co. Inc., Indiana, USA. UV−vis spectra were recorded on a Hitachi U-3000 spectrometer. Photovoltaic devices were prepared onto pre-etched and cleaned, patterned FTO substrates. The TiO_2 blocking layer was deposited *via* spray pyrolysis deposition using a TiO_2 precursor, TAA, diluted with ethanol to a concentration of 0.2 M. The pyrolysis was carried out at 480 °C. After the required number of spraying cycles under optimized conditions,[31] the substrates were annealed at 500 °C for another hour before cooling down to room temperature. The substrates were kept in an inert atmosphere for further layer preparation. The active layers were processed *via* the doctor-blading technique using a Coatmaster 509 MC-I Film Applicator from Erichsen GmbH & Co. KG, Germany. Films were processed at ambient conditions and the processing speed was 25 mm s^{-1} for all films. The films were dried at ambient conditions for 1 h. Three types of film application blades, (a) spiral film applicator blade, model 358, (20 μm blade gap), (b) quadruple film applicator model 360 (120 μm blade gap) and (c) film applicator blade BAKER 286 (5 μm blade gap) (Erichsen GmbH & Co. KG) were used for optimization of the optical quality of the films. The best method for the preparation of PBI−xerogel and PBI−xerogel/*p*vDMTPD blend layers was found to be that using spiral film applicator blade. All films were prepared from 30 μL hot (~55 °C) 2.0 wt % $CHCl_3$ solutions resulting in 160 nm thick blend films. The additional overstanding *p*vDMTPD layer was prepared with the film applicator blade BAKER 286 (5 μm blade gap) from 10 μL 5.0 wt % chlorobenzene solution to get 140 nm smooth films. Film thicknesses were measured with a Dek Tak 3030 ST profilometer from Veeco Intruments. PEDOT:PSS dispersion, obtained from Aldrich, was spin-coated (4000 rpm, ramp 1 s, 90 s) and postbaked on a hot-stage at 80 °C for 10 min in a nitrogen atmosphere. The gold electrode (60 nm) was deposited by vacuum sublimation in a vacuum chamber of BA 510 type from Balzers (Liechtenstein) at 10^{-6} mbar. The active area of the cells was 0.12 cm^2. Current−voltage characteristics were measured under 100 mW cm^{-2} and AM 1.5 spectral light (Oriel light source setup with 150-W xenon arc lamp and suitable AM 1.5 filters). This setup was calibrated using a reference Si cell from ISE Freiburg at the same sample position and height. Samples for SEM were prepared on FTO substrates under the same conditions as those used for solar cell preparation and sputtered with platinum (2 nm) to improve the conductivity for SEM imaging. The measurements were performed with a LEO 1530 (FE-SEM) with Schottky-field-emission cathode and in-lens detector. AFM measurements were performed with a Dimension 3100 device from Digital Instruments. Images were recorded in the tapping mode.

Acknowledgment. Financial Support from DFG (SPP 1355 and SFB 481) is acknowledged. Dr. S. Ghosh thanks the Alexander von Humboldt foundation for a postdoctoral fellowship.

REFERENCES AND NOTES

1. Günes, S.; Neugebauer, H.; Sariciftci, N. S. Conjugated Polymer-Based Organic Solar Cells. *Chem. Rev.* **2007**, *107*, 1324−1338.
2. Hoppe, H.; Sariciftci, N. S. Polymer Solar Cells. In *Advances in Polymer Science Photoresponsive Polymers II*; Marder, S. R., Lee, K.-S., Eds.; Springer-Verlag: Heidelberg, Germany, 2008; pp 1−86.
3. Brabec, C. J.; Sariciftci, N. S.; Hummelen, J. C. Plastic Solar Cells. *Adv. Funct. Mater.* **2001**, *11*, 15–26.
4. Halls, J. J. M.; Walsh, C. A.; Greenham, N. C.; Marseglia, E. A.; Friend, R. H.; Moratti, S. C.; Holmes, A. B. Efficient Photodiodes from Interpenetrating Polymer Networks. *Nature* **1995**, *376*, 498–500.
5. Yang, X.; Loos, J. Toward High-Performance Solar Cells: The Importance of Morphology Control. *Macromolecules* **2007**, *40*, 1353–1362.
6. Ma, W.; Yang, C.; Gong, X.; Lee, K.; Heeger, A. J. Thermally Stable, Efficient Polymer Solar Cells with Nanoscale Control of the Interpenetrating Network Morphology. *Adv. Funct. Mater.* **2005**, *15*, 1617–1622.
7. Lindner, S. M.; Hüttner, S.; Chiche, A.; Thelakkat, M.; Krausch, G. Charge Separation at Self-Assembled Nanostructured Bulk Interface in Block Copolymers. *Angew. Chem., Int. Ed.* **2006**, *45*, 3364–3368.
8. Sommer, M.; Lindner, S. M.; Thelakkat, M. Microphase-Separated Donor−Acceptor Diblock Copolymers: Influence of HOMO Energy Levels and Morphology on Polymer Solar Cells. *Adv. Funct. Mater.* **2007**, *17*, 1493–1500.
9. Cravino, A.; Zerza, G.; Maggini, M.; Bucella, S.; Svensson, M.; Andersson, M. R.; Neugebauer, H.; Sariciftci, N. S. A Novel Polythiophene with Pendant Fullerenes: Toward Donor/Acceptor Double-Cable Polymers. *Chem. Commun.* **2000**, 2487–2488.
10. Würthner, F.; Chen, Z.; Hoeben, F. J. M.; Osswald, P.; You, C.-C.; Jonkheijm, P.; van Herrikhuyzen, J.; Schenning, A. P. H. J.; van der Schoot, P. P. A. M.; Meijer, E. W.; Beckers, E. H. A.; Meskers, S. C. J.; Janssen, R. A. J. Supramolecular p−n-Heterojunctions by Co-Self-Organization of Oligo(*p*-phenylene vinylene) and Perylene Bisimide Dyes. *J. Am. Chem. Soc.* **2004**, *126*, 10611–10618.
11. McClenaghan, N. D.; Grote, Z.; Darriet, K.; Zimine, M.; Williams, R. M.; De Cola, L.; Bassani, D. M. Supramolecular Control of Oligothienylenevinylene−Fullerene Interactions:Evidence for a Ground-State EDA Complex. *Org. Lett.* **2005**, *7*, 807–810.
12. Sisson, A. L.; Sakai, N.; Banerji, N.; Fürstenberg, A.; Vauthey, E.; Matile, S. Zipper Assembly of Vectorial Rigid-Rod π-Stack Architectures with Red and Blue Naphthalenediimides: Toward Supramolecular Cascade n/p-Heterojunctions. *Angew. Chem., Int. Ed.* **2008**, *47*, 3727–3729.

13. Haryono, A.; Binder, W. H. Controlled Arrangement of Nanoparticle Arrays in Block-Copolymer Domains. *Small* **2006**, *2*, 600–611.
14. Terech, P.; Weiss, R. G. Low Molecular Mass Gelators of Organic Liquids and the Properties of Their Gels. *Chem. Rev.* **1997**, *97*, 3133–3159.
15. Hirst, A. R.; Escuder, B.; Miravet, J. F.; Smith, D. K. High-Tech Applications of Self-Assembling Supramolecular Nanostructured Gel-Phase Materials: From Regenerative Medicine to Electronic Devices. *Angew. Chem., Int. Ed.* **2008**, *47*, 8002–8018.
16. Puigmartí-Luis, J.; Laukhin, V.; Pérez del Pino, A.; Vidal-Gancedo, J.; Rovira, C.; Laukhina, E.; Amabilino, D. B. Supramolecular Conducting Nanowires from Organogels. *Angew. Chem., Int. Ed.* **2007**, *46*, 238–241.
17. Lee, D.-C.; Jang, K.; McGrath, K. K.; Uy, R.; Robins, K. A.; Hatchett, D. W. Self-Assembling Asymmetric Bisphenazines with Tunable Electronic Properties. *Chem. Mater.* **2008**, *20*, 3688–3695.
18. Hüttner, S.; Sommer, M.; Thelakkat, M. N-type Organic Field Effect Transistors from Perylene Bisimide Block Copolymers and Homopolymers. *Appl. Phys. Lett.* **2008**, *92*, 093302.
19. Thelakkat, M. Star-Shaped, Dendrimeric and Polymeric Triarylamines as Photoconductors and Hole Transport Materials for Electro-optical Applications. *Macromol. Mater. Eng.* **2002**, *287*, 442–461.
20. *Semiconducting Polymers. Chemistry, Physics and Engineering*; Hadziioannou, G., Malliaras, G. G., Eds.; Wiley-VCH: Weinheim, Germany, 2007.
21. Dittmer, J. J.; Marseglia, E. A.; Friend, R. H. Electron Trapping in Dye/Polymer Blend Photovoltaic Cells. *Adv. Mater.* **2000**, *12*, 1270–1274.
22. Breeze, A. J.; Salomon, A.; Ginley, D. S.; Tillmann, H.; Hörhold, H.-H.; Gregg, B. A. Polymer−Perylene Diimide Heterojunction Solar Cells. *Appl. Phys. Lett.* **2002**, *81*, 3085–3087.
23. Shin, W. S.; Jeong, H.-H.; Kim, M.-K.; Jin, S.-H.; Kim, M.-R.; Lee, J.-K.; Lee, J. W.; Gal, Y.-S. Effects of Functional Groups at Perylene Diimide Derivatives on Organic Photovoltaic Device Application. *J. Mater. Chem.* **2006**, *16*, 384–390.
24. Mohmeyer, N.; Wang, P.; Schmidt, H.-W.; Zakeeruddin, S. M.; Grätzel, M. Quasi-Solid-State Dye-Sensitized Solar Cells with 1,3:2,4-Di-*O*-benzylidene-D-sorbitol Derivatives as Low Molecular Weight Organic Gelators. *J. Mater. Chem.* **2004**, *14*, 1905–1909.
25. Kubo, W.; Kitamura, T.; Hanabusa, K.; Wada, Y.; Yanagida, S. Quasi-Solid-State Dye-Sensitized Solar Cells Using Room Temperature Molten Salts and a Low Molecular Weight Gelator. *Chem. Commun.* **2002**, 374–375.
26. Würthner, F.; Bauer, C.; Stepanenko, V.; Yagai, S. A Black Perylene Bisimide Super Gelator with an Unexpected *J*-Type Absorption Band. *Adv. Mater.* **2008**, *20*, 1695–1698.
27. Ghosh, S.; Li, X.-Q.; Stepanenko, V.; Würthner, F. Control of *H*- and *J*-Type π-Stacking by Peripheral Alkyl Chains and Self-Sorting Phenomena in Perylene Bisimide Homo- and Heteroaggregates. *Chem.—Eur. J.* **2008**, *14*, 11343–11357.
28. Lindner, S. M.; Thelakkat, M. Nanostructured n-type Organic Semiconductor in a p-type Matrix *via* Self-Assembly of Block Copolymers. *Macromolecules* **2004**, *37*, 8832–8835.
29. Moffat, J. R.; Smith, D. K. Metastable Two-Component Gel-Exploring The Gel-Crystal Interface. *Chem. Commun.* **2008**, 2248–2250.
30. Ballabh, A.; Adalder, T. K.; Dastidar, P. Structures and Gelation Properties of a Series of Salts Derived from an Acyclic Dicarboxylic Acid and *n*-Alkyl Primary Amines. *Cryst. Growth Des.* **2008**, *8*, 4144–4149.
31. Peng, B.; Jungmann, G.; Jäger, C.; Haarer, D.; Schmidt, H.-W.; Thelakkat, M. Systematic Investigation of the Role of Compact TiO_2 Layer in Solid-State, Dye-Sensitized TiO_2 Solar Cells. *Coord. Chem. Rev.* **2004**, *248*, 1479–1489.